

Chapter 32

Imaging and Focusing Through Scattering Medium Based on Reflection Matrix Optical Coherence Tomography



Jing Cao and Pinghe Wang

Abstract Multiple scattering inside the random medium limits the imaging depth of optical coherence tomography (OCT) to 1–2 mm, as well as the degree of focus at the deep imaging depth. In this paper, by combining the concept of matrix measurement with a wide-field optical coherence tomography, we have done two aspects of work. The first one is for deeper imaging depth. By reconstructing the huge reflection matrix of the sample and then applying a time-reversal operation to it, we successfully filter out the single scattered light for imaging at the depth of 15 times of the scattering mean free path (SMFP). Since the imaging depth of conventional OCT is 6–7 times of the SMFP, our proposed reflection matrix optical coherence tomography (RMOCT) is about one time deeper than the conventional OCT. The second part of the work is a high-speed wavefront shaping (WFS) method based on a one-time in-and-out complex light field analysis. With the help of a phase-only spatial light modulator, we realize the light focusing through a random medium is ~ 113 ms. It is about three times faster than the iterative feedback wavefront shaping method. We believe that our work might pave the way to apply WFS to optical imaging methods and open new methods toward deeper imaging through a scattering medium.

32.1 Introduction

Because of multiple scattering, the propagation of light in random media poses a fundamental problem in optical imaging technologies. The challenge becomes much more difficult when considering obtaining mesoscopic-level resolution in a scattering media. Most of the optical imaging methods still rely on the collection of ballistic light to construct the sample information, such as conventional microscopy imaging. They provide diffraction-limited resolution but image penetration is limited to a superficial level. This is because the amount of ballistic (or single scattering) light decreases exponentially with the penetration depth. At present, one method to overcome this is to take advantage of diffuse light reflected back from the layers

J. Cao (✉) · P. Wang

School of Optoelectronic Science and Engineering, University of Electronic Science and Technology of China, Chengdu 610054, China

deep inside the tissue, such as diffuse optical tomography, acousto-optic imaging, and photoacoustic imaging. But their resolutions are severely degraded because they rely on diffused light to form an image. In modern optical society, there are two techniques to discriminate single scattering light from the multiple scattering light for high-resolution imaging capacity. The first option is confocal grating technology, such as confocal microscopy [1] or two-photon microscopy [2–4], which spatially rejects unwanted multiple scattering light based on the spatial filter. Another option is the coherence grating method, such as optical coherence tomography [5, 6], which extracts single scattering light based on the path length they travel in tissue. The combining of these two gates together, optical coherence microscopy [7, 8], can be stronger than either gate individually, achieving greater image penetration in scattering medium without compromising the imaging resolution.

Either for optical imaging or focusing purpose, a lot of remarkable works have been done to break through the limitation caused by multiple scattering. The light manipulation method was proposed [9], known as wavefront shaping, to focus light through a highly scattering medium with the help of a spatial light modulator [10–12]. There have been many remarkable signs of progress such as the investigation of transmission matrix to describe the light propagation in a complex medium [13–16] and the presence of reflection matrix method to imaging through highly scattering tissue [17–20].

In this paper, we have demonstrated a reflection matrix OCT, which has the imaging ability of 15 times of the SMFP. At the same time, by using the lock-in detection instead of the four-step phase-shift method, the acquisition speed of each scanning point has been accelerated to 0.37 s. It is about ten times faster than the previous four-step phase-shift method (4.15 s for each scanning point). Then, we configured the sample arm to a transmitted mode for light focusing purposes. Based on a high-speed and high-sensitivity complex light field reconstruction technology, we realize the light focusing through the sample at the speed of ~ 113 ms.

32.2 Methods

32.2.1 Experimental Setup

The experimental setup to record the sample's reflection matrix is depicted in Fig. 32.1. A femtosecond laser with center wavelength $\lambda_0 = 790$ nm and spectrum bandwidth $\Delta\lambda = 90$ nm is first collimated and expanded by a pair of lenses. After passing through a beam splitter (BS1), the beam splits into the sample arm and reference arm.

In the reference arm, optical frequency is shifted to $f_0 + f_r$, where f_0 is the center frequency of the laser and f_r is the frequency difference of the two acousto-optic modulators (AOM). In our case, f_r is 40 kHz. After passing through another pair of lenses and pinhole, BS2, PBS2, and a mirror, the reference light is then reflected

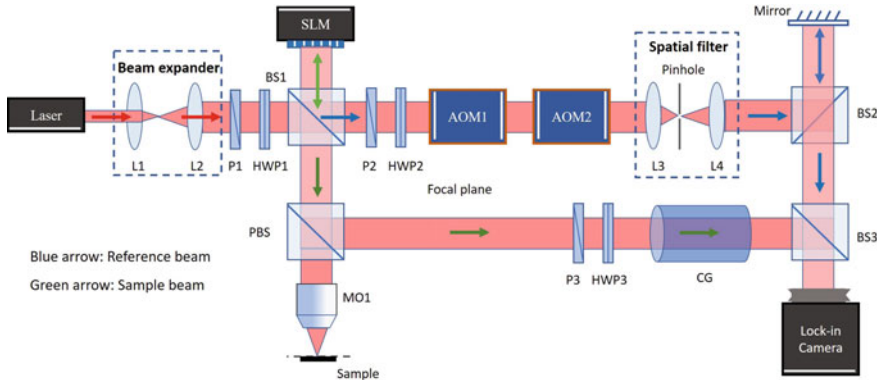


Fig. 32.1 Experimental setup for the measurement of RM

back at BS3. In the sample arm, the phase of the beam is shaped by a spatial light modulator (PLUTO-2, HOLOEYE) operating at phase-only mode, and subsequently transmitted through the BS1 again. After passing through a PBS1 and a QWP oriented at 45° , it focuses onto the sample through a microscope objective (MO). In order to detect the phase of the sample, a piece of compensation glass has been used to match the dispersion introduced by the two AOMs in the reference arm. Finally, the interference signal will be detected by the lock-in camera. The benefit of using this type of camera is that it can directly output two components, in-phase (I) and quadrature (Q), to form the complex light field.

32.2.2 Time-Reversal Operation for Imaging Through Scattering Medium

In this setup, we apply a point-to-point scanning strategy to collect the sample information. For each scanning point, there will be a 2D matrix filled with complex light field information. Then, we reshape it into a 1D vector and fill it into one column of the RM. After finishing all the scanning and repeating this filling process, we achieve a huge matrix, the so-called reflection matrix. By using the singular value decomposition and time-reversal operation [21, 22], it is able to restore the imaging of the target beneath the scattering layer.

32.2.3 Wavefront Shaping for Focusing Light Through Scattering Medium

For light focusing purposes, we have changed the configuration of the sample arm into a transmitted mode, as shown in Fig. 32.2. Light from the first microscopy (M1) focused onto the front of the sample and the transmitted light would be collected by the second microscopy (M2).

As shown in Fig. 32.3, it is the basis of our proposed high-speed wavefront method. In Fig. 32.3a, a plane wave incidents onto a scattering medium, the output beam forms a speckle pattern. Based on the fact that there always exists an optimal wavefront, by shaping the incident light to this wavefront, the transmitted light will become all in phase again. Equation (32.1) shows how to calculate this optimal wavefront:

$$O_{in} = E_{in} * E_{out}^{-1} * E_{in} \tag{32.1}$$

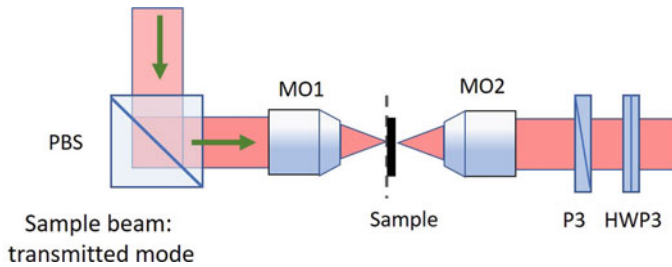


Fig. 32.2 Experimental setup for focusing light

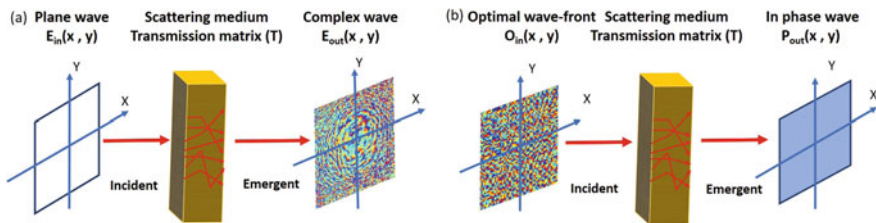


Fig. 32.3 Principle of high-speed wavefront shaping

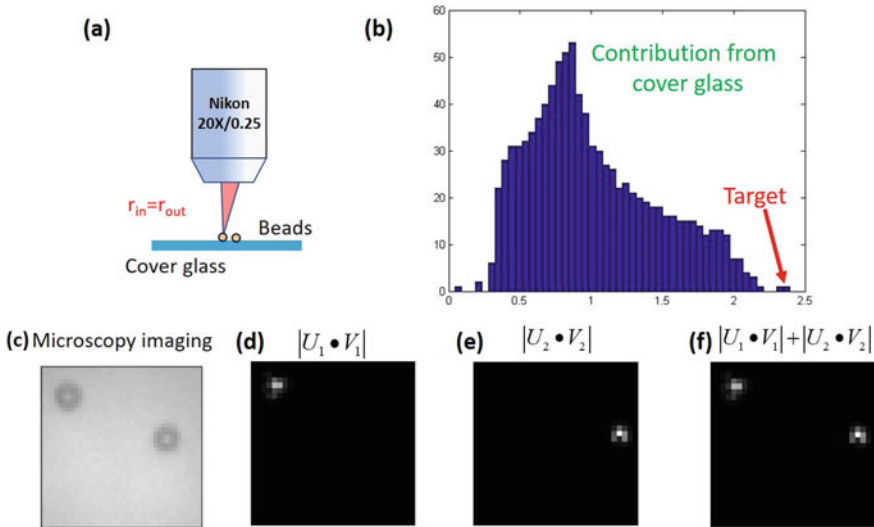


Fig. 32.4 Imaging at the single scattering region

32.3 Results and Discussion

32.3.1 Imaging at the Single Scattering Region

At this step, the imaging target is two beads attached to cover glass and there is no scattering layer (as shown in Fig. 32.4a). Figure 32.4b shows the distribution of singular values. We can see the singular values that have the first two corresponding to the imaging targets. Figure 32.4c is the microscopy image of the target for comparison purposes. Figure 32.4d–f shows the recovered images by using the first singular vector, second singular vector, and the first two singular vectors, respectively.

32.3.2 Imaging at Multiple Scattering Regions

This time, we have inserted a high scattering layer, a piece of A4 paper sheet, between the microscopy and the cover glass (as shown in Fig. 32.5a). The thickness of the sheet is $97 \mu\text{m}$ and the SMFP is $6.4 \mu\text{m}$, which means the optical thickness of the scattering layer is 15.2 SMFP. Figure 32.5b shows the distribution of singular values. We can see the singular values that have the first two corresponding to the imaging targets. Figure 32.5c–e shows the recovered images by using the first singular vector, second singular vector, and the first two singular vectors, respectively. Based on the above results, the RMOCT presents its ability to imaging ability through 15.2 SMFP.

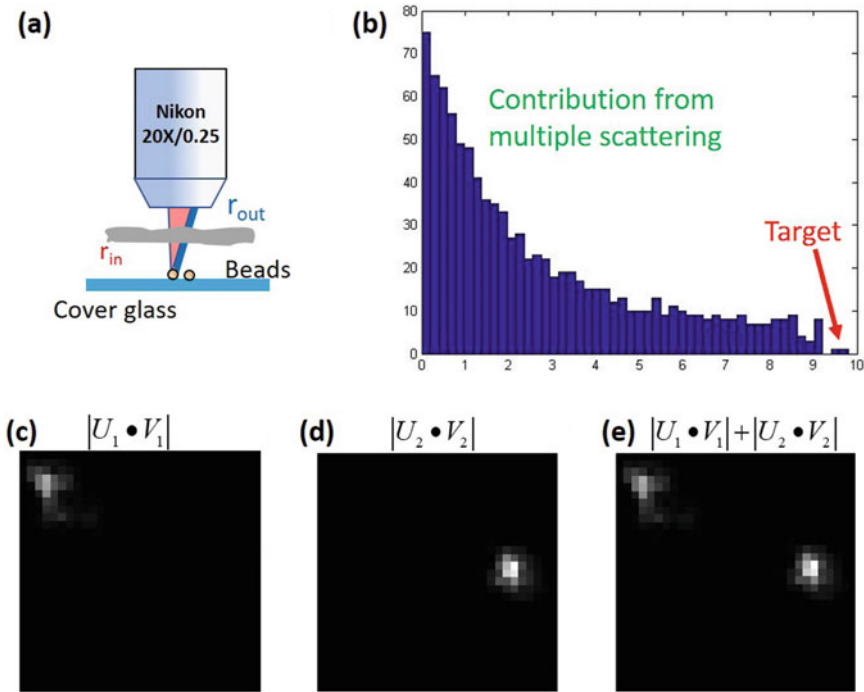


Fig. 32.5 Imaging at multiple scattering regions

32.3.3 Imaging Through a Thick Biological Sample

We have home-made a highly scattering layer (0.8 mm thickness phantom) by adding 20 g titanium dioxide into a 100 g silicone rubber base. The imaging target this time is a polydimethylsiloxane (PDMS) material, which is soft and flexible. Figure 32.6a is the sample setup. We use a water immersion objective with a bigger numerical aperture this time. Figure 32.6b shows the distribution of singular values in decreasing order. Figure 32.6c is the microscopy imaging of the PDMS material. Figure 32.6d and e shows the recovered images by using the first 38 singular vectors at the situation without and with scattering later, respectively.

In order to show the power imaging ability of RMOCT, we use a commercial 1.3 μm swept-source OCT from Thorlabs Inc. to image the same sample. The results are shown in Fig. 32.7. Figure 32.7a is the imaging result of PDMS material without the scattering layer. We can see the boundaries are very clear. Figure 32.7b is the *en-face* imaging of the upper layer. Figure 32.7c is the imaging result of PDMS material beneath the scattering layer, and we can see the boundaries are blurry. Figure 32.7d is the *en-face* imaging of the upper layer of PDMS material. This time, the commercial OCT system lost the ability to recover the image.

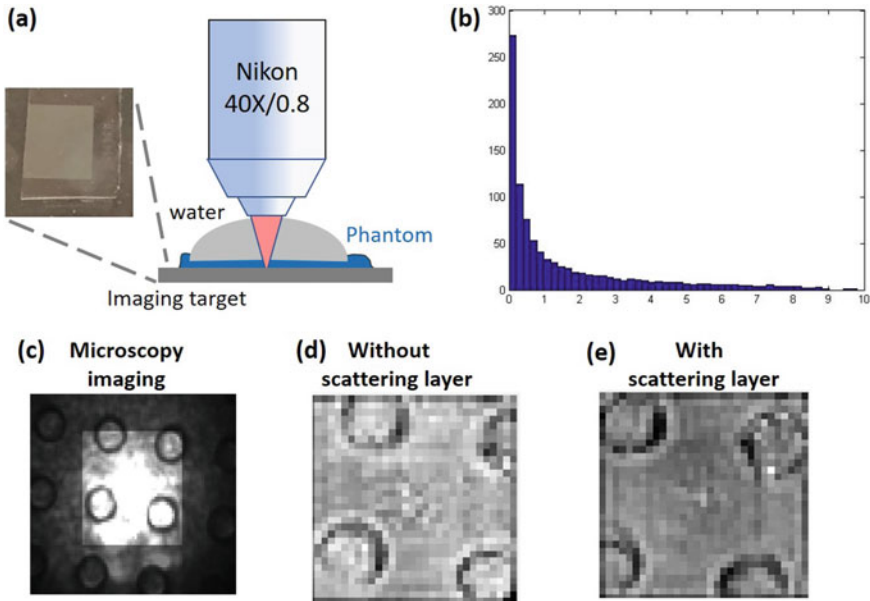


Fig. 32.6 Imaging through a thick biological sample

32.3.4 High-Speed Wavefront Shaping

As for the light focusing experiment, the phase and amplitude before wavefront are all made of chaos. However, the phase and amplitude after wavefront have been shaped to a Gaussian-like distribution. The whole process only needs 133 ms.

32.4 Conclusions

In this paper, we have demonstrated a new type of OCT combined with reflection matrix measurement. The huge reflection matrix of the sample contains abundant information which describes the light propagation process within the sample. We have presented its amazing imaging power at deeper penetration depth, which is 15 times MSFP and two times the conventional OCT's imaging depth. At the same time, we have shown a high-speed WFS method to focus light through a sample in ~133 ms. As a next step, we are now trying to apply WFS technology to OCT to realize deeper imaging depth.

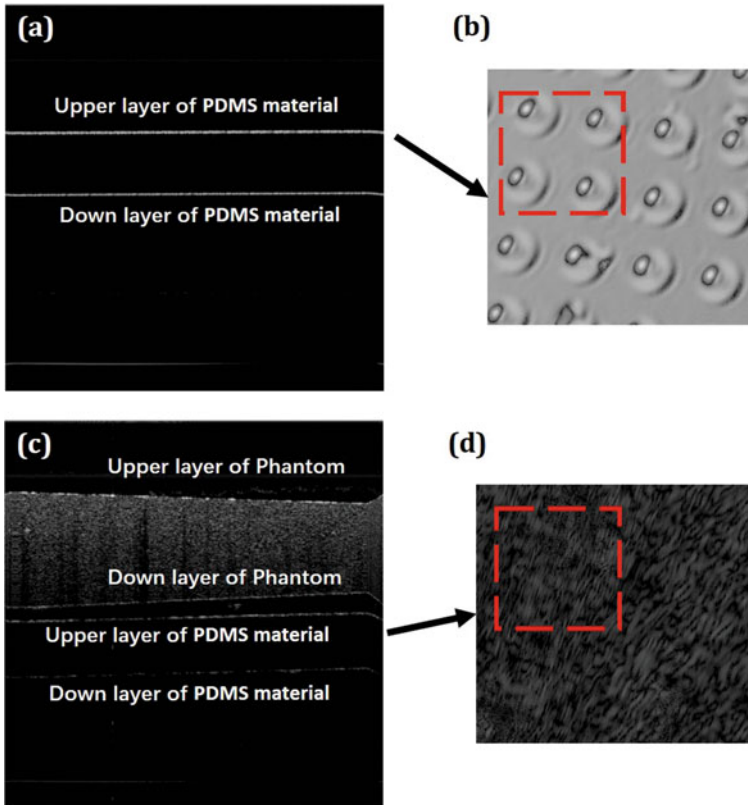


Fig. 32.7 Imaging results of a commercial 1.3 μm swept-source OCT

Acknowledgements This research was financially supported by the National Key R&D Program of China (Grant No. 2016YFF0102003).

References

1. G.J. Tearney, R.H. Webb, B.E. Bouma, Spectrally encoded confocal microscopy. *Opt. Lett.* **23**(15), 1152–1154 (1998)
2. T. Liu, X. Zhang, Q. Qiao, C. Zou, L. Feng, J. Cui, Z. Xu, A two-photon fluorescent probe for imaging hydrogen sulfide in living cells. *Dyes Pigm.* **99**(3), 537–542 (2013)
3. P.J. Campagnola, L.M. Loew, Second-harmonic imaging microscopy for visualizing biomolecular arrays in cells, tissues and organisms. *Nat. Biotechnol.* **21**(11), 1356 (2003)
4. H. Cui, C. Hua, P. Yue, W. Lin, A two-photon fluorescent turn-on probe for palladium imaging in living tissues. *Sens. Actuators B Chem.* **219**, 232–237 (2015)
5. J. Jang, J. Lim, H. Yu, H. Choi, Y. Park, Complex wavefront shaping for optimal depth-selective focusing in optical coherence tomography. *Opt. Express* **21**(3), 2890–2902 (2013)

6. H. Yu, J. Jang, J. Lim, J.H. Park, W. Jang, J.Y. Kim et al., Depth-enhanced 2-D optical coherence tomography using complex wavefront shaping. *Opt. Express* **22**(7), 7514–7523 (2014)
7. J. Liang, L. Zhu, L.V. Wang, Single-shot real-time femtosecond imaging of temporal focusing. *Light Sci. Appl.* **7**(005), 466–475 (2018)
8. J.H. Park, C. Park, H.S. Yu, J. Park, S. Han, J. Shin et al., Subwavelength light focusing using random nanoparticles. *Nat. Photonics* **7**(6), 454–458 (2013)
9. I.M. Vellekoop, A.P. Mosk, Focusing coherent light through opaque strongly scattering media. *Opt. Lett.* **32**(16), 2309 (2007)
10. A.S. Hemphill, Y. Shen, L. Yan, L.V. Wang, High-speed single-shot optical focusing through dynamic scattering media with full-phase wavefront shaping. *Appl. Phys. Lett.* **111**(22), 221109 (2017)
11. M. Hacker, G. Stobrawa, R. Sauerbrey, T. Buckup, M. Motzkus, M. Wildenhain et al., Micromirror SLM for femtosecond pulse shaping in the ultraviolet. *Appl. Phys. B* **76**(6), 711–714 (2003)
12. O. Katz, E. Small, Y. Bromberg, Y. Silberberg, Focusing and compression of ultrashort pulses through scattering media. *Nat. Photonics* **5**(6), 372–377 (2011)
13. M. Cui, A high speed wavefront determination method based on spatial frequency modulations for focusing light through random scattering media. *Opt. Express* **19**(4), 2989 (2011)
14. H.P. Paudel, C. Stockbridge, J. Mertz, T. Bifano, Focusing polychromatic light through scattering media, in *Mems Adaptive Optics VII* (International Society for Optics and Photonics)
15. J. Aulbach, B. Gjonaj, P. Johnson, A. Lagendijk, Spatiotemporal focusing in opaque scattering media by wave front shaping with nonlinear feedback. *Opt. Express* **20**(28), 29237 (2012)
16. D. Wang, E.H. Zhou, J. Brake, H. Ruan, M. Jang, C. Yang, Focusing through dynamic tissue with millisecond digital optical phase conjugation. *Optica* **2**(8), 728–735 (2015)
17. B. Zhuang, C. Xu, Y. Geng, G. Zhao, H. Chen, Z. He, L. Ren, An Early study on imaging 3D objects hidden behind highly scattering media: a round-trip optical transmission matrix method. *Appl. Sci.* **8**(7), 1036 (2018)
18. A. Aubry, A. Derode, Detection and imaging in a random medium: A matrix method to overcome multiple scattering and aberration. *J. Appl. Phys.* **106**(4) (2009)
19. C. Xu, B. Zhuang, Y. Geng, H. Chen, L. Ren, Z. Wu, A scanning-free wide-field single-fiber endoscopic image retrieval method based on optical transmission matrix. *Laser Phys.* **29**(4) (2019)
20. Y. Choi, T.R. Hillman, W. Choi, N. Lue, R.R. Dasari, P.T.C. So et al., Measurement of the time-resolved reflection matrix for enhancing light energy delivery into a scattering medium. *Phys. Rev. Lett.* **111**(24), 243901 (2013)
21. A. Badon, D. Li, G. Lerosey, A.C. Boccara, M. Fink, A. Aubry, Smart optical coherence tomography for ultra-deep imaging through highly scattering media. *Sci. Adv.* **2**(11) (2016)
22. Q. Yang, J. Cao, Y. Miao, J. Zhu, Z. Chen, Extended imaging depth of en-face optical coherence tomography based on fast measurement of reflection matrix by widefield heterodyne detection. *Opt. Lett.* **45**(4) (2019)